Aerosol and Air Quality Research, 14: 533–549, 2014

ISSN: 1680-8584 print / 2071-1409 online
doi: 10.4209/aaqr.2013.09.0283

Comparison of CO_2 Photoreduction Systems: A Review

Wei-Ning Wang[1], Johnathon Soulis[1], Y. Jeffrey Yang[2], Pratim Biswas[1*]

[1] *Aerosol and Air Quality Research Laboratory, Department of Energy, Environmental and Chemical Engineering, Washington University in St. Louis, St. Louis, MO 63130, USA*
[2] *Office of Research and Development, National Risk Management Research Laboratory, U.S. Environmental Protection Agency, Cincinnati, OH 45268, USA*

ABSTRACT

Carbon dioxide (CO_2) emissions are a major contributor to the climate change equation, and thus strategies need to be developed in order to reduce increases in CO_2 levels in the atmosphere. One of the most promising approaches is to convert CO_2 into useful products in engineered processes. The photocatalytic reduction of CO_2 into hydrocarbon fuels is a promising way to recycle CO_2 as a fuel feedstock by taking advantage of the readily available solar energy. This article reviews the basics of CO_2 photoreduction mechanisms, limiting steps, possible strategies to enhance photoreduction efficiency, and the state-of-the-art photocatalytic systems for CO_2 reduction. In particular, a comparison between different catalytic systems, including biological (plants and algae), inorganics (semiconductors), organics (molecular complexes), and hybrid (enzyme/semiconductors) systems is provided.

Keywords: Fossil fuels; Global warming; Photocatalysis; Solar energy; Nanotechnology.

INTRODUCTION

Fossil fuels, such as coal, petroleum, and natural gas, are the major conventional energy sources in the world due to their availability, stability, and high energy density (Roy *et al.*, 2010; Biswas *et al.*, 2011). The continuous reliance on burning fossil fuels has raised atmospheric carbon dioxide (CO_2) levels by approximately 100 parts per million (ppm) by volume over the last century (Metz *et al.*, 2005). CO_2 emissions are widely considered as the major cause of global warming. Thus there is an increasing need to mitigate CO_2 emissions. In June 2013, the U.S. President Barack Obama announced a plan to address climate change brought upon by CO_2 emissions. A proposal to regulate anthropogenic CO_2 emissions from existing and future electricity generating power plants as a part of a greater initiative to reduce and displace CO_2 emissions globally was suggested. Several strategies to accomplish this are being considered. Among them, carbon capture and sequestration (CCS) technologies are generally considered as an efficient and viable method to mitigate CO_2 emissions. CO_2 mitigation by these CCS technologies can be realized by pre-, post-, and oxy-fuel combustion technologies, which can be followed by compression and geological sequestration. However, these technologies require high energy inputs and are generally high cost, making it economically disincentive for widespread use at its current stage of development.

As fossil fuels will continue to be used globally in the near future, it is imperative to consider efficient CO_2 mitigation methodologies. While CCS sequestration in geological formations will be essential due to the necessary large scale of CO_2 emission reductions; it is also important to evaluate methodologies for conversion of the captured CO_2 to useful products and promoting use of carbon neutral methodologies. Carbon dioxide reduction can be realized by several different ways, such as biological reduction by plants (Blankenship *et al.*, 2011), and thermal (Chueh and Haile, 2009), electrochemical (Abe *et al.*, 1996; Jitaru *et al.*, 1997), or photocatalytic reduction (Inoue *et al.*, 1979) using synthetic systems. Among these options, CO_2 photoreduction is gaining increasing attention since it can potentially consume alternative forms of energy by harnessing solar energy, which is abundant, cheap, and ecologically clean and safe. In a typical semiconductor-based photocatalyst system, the catalyst needs to absorb light energy, generate electron-hole pairs, spatially separate them and transfer them to redox active species across the interface (Fujishima *et al.*, 2008). In spite of its economic and environmental benefits, the photocatalytic pathways, however, are very complex and always suffer from low efficiency due to several limiting factors, such as fast electron-hole (e^--h^+) recombination rates, complicated backward reactions, narrow

* Corresponding author.
Tel.: 1-314-935-5548; Fax: 1-314-935-5464
E-mail address: pbiswas@wustl.edu

light absorption wavelength range (in particular to wide bandgap semiconductors such as titania (TiO_2) and zinc oxide (ZnO)), and low CO_2 affinity of the photocatalysts.

There are several reviews on CO_2 photoreduction (Sutin *et al.*, 1997; Song, 2006; Usubharatana *et al.*, 2006; Kitano *et al.*, 2007; Indrakanti *et al.*, 2009; Morris *et al.*, 2009; Dorner *et al.*, 2010; Roy *et al.*, 2010; Biswas *et al.*, 2011; Windle and Perutz, 2012; Hong *et al.*, 2013), covering both fundamental CO_2 photoreduction mechanisms and practical photocatalyst development. This article intends to provide a state-of-the-art overview of the basics of CO_2 photoreduction pathways, and a comparison of different CO_2 photoreduction systems as listed below: (1) Biological systems, including mainly algae; (2) Inorganic photocatalysts, mostly transition metal oxides (or semiconductors), in particular TiO_2-based catalysts; (3) Organic photocatalysts, including mainly metal-organic complexes; and (4) inorganic and organic/biological hybrid, or the so-called biomimetic systems, consisting of enzyme-activated or dye-sensitized semiconductors. A summary and outlook of CO_2 photoreduction have been made for future development of efficient photocatalytic systems.

BASICS OF CO_2 PHOTOREDUCTION SYSTEMS

Typical Mechanisms

The mechanism of CO_2 photoreduction occurs through a set of complicated steps. Taking semiconductor photocatalysts as an example, to reduce CO_2, the semiconductor should be activated by light with the energy (E_{hv}) equal to or higher than its bandgap (E_g) (e.g., $E_{hv} \geq$ 3.2 eV for anatase TiO_2). The bandgap excitation (photoexcitation) leads to the formation of electrons in conduction band (CB) and holes in valence band (VB), which serve as the sites for photoreduction and photooxidation, respectively. The catalyst is also required to have its electrons with higher energy compared to the corresponding CO_2 reduction potential. In an ideal system, this means that the CB potential (or the so-called band edge) of the catalyst should be well above (more negative than) the reduction potential for a certain product at a predetermined pH. Meanwhile, the holes should be able to oxidize water to O_2 and produce protons (H^+), i.e., the VB edge should be well below (more positive than) the water oxidation level for an efficient photolysis. Fig. 1 shows the energy levels of several semiconductors and the corresponding redox potentials in the CO_2 photoreduction system (Inoue *et al.*, 1979).

The possible reactions that can occur in the reduction of CO_2 in aqueous medium are shown in Scheme 1 (Inoue *et al.*, 1979; Sutin *et al.*, 1997; Fujita 1999; Usubharatana *et al.*, 2006; Indrakanti *et al.*, 2009). It is apparent from Scheme 1 that CO_2 photoreduction involves multiple steps. As explained above, the initial step in the photocatalytic reduction of CO_2 is the generation of e^--h^+ pairs (Eq. (1)). After photoexcitation, the e^--h^+ pairs should be separated spatially, and be transferred to redox active species across the interface and minimize electron hole recombination. Fig. 2 shows the possible charge transfer pathways of the TiO_2 photocatalyst (Fujishima *et al.*, 2008), which involves several critical charge transfer steps. Lifetime of the e^--h^+ pairs is only a few nanoseconds, but this is adequate for promoting redox reactions. However, the time scale of e^--h^+ recombination (Eq. (2)) is two or three orders of magnitude faster than other electron transfer processes (Indrakanti *et al.*, 2009). This is thus considered as one of the major limiting steps in photocatalysis. Therefore, any process which inhibits e^--h^+ recombination would greatly increase the efficiency and improve the rates of CO_2 photoreduction.

Ideally, after photoexcitation, water (or other hole scavengers if not in aqueous systems) is oxidized by holes to form oxygen and protons (H^+) (Eq. (3)), which are essential

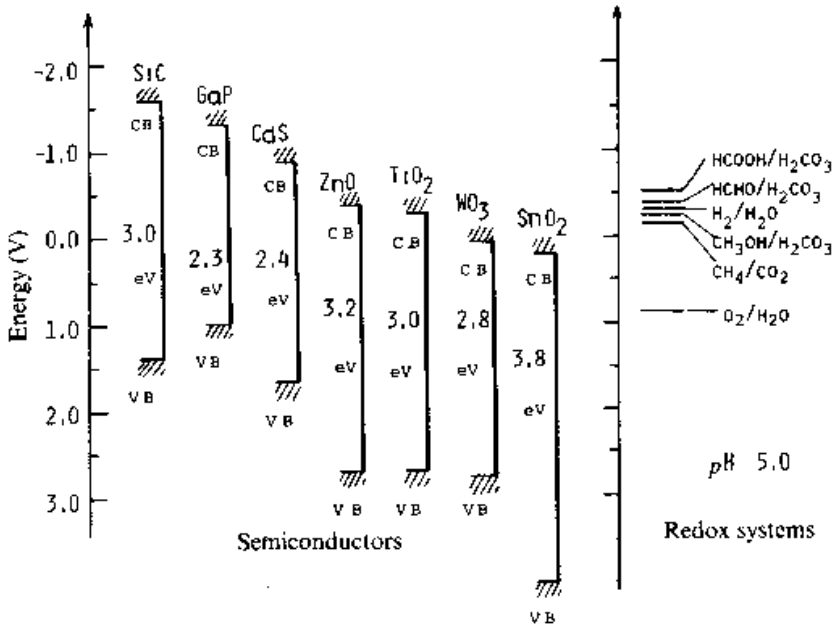

Fig. 1. Schematic diagram of the energy correlation between semiconductor catalysts and redox couples in water at pH = 5. (Reprinted with permission from Inoue *et al.*, 1979; Copyright 1979 Nature Publishing Group).

Photocatalyst + $h\nu \rightarrow e^- + h^+$	(1)	
$e^- + h^+ \rightarrow$ heat (recombination)	(2)	
Photooxidation reactions		
Water oxidation/decomposition		$E°_{redox}$/V vs. NHE
$H_2O + 2h^+ \rightarrow 1/2O_2 + 2H^+$	(3)	= 0.82
Hydrogen peroxide formation		
$O_2 + 2H^+ + 2e^- \rightarrow H_2O_2$	(4)	
Photoreduction reactions		
Hydrogen formation		$E°_{redox}$/V vs. NHE
$2H^+ + e^- \rightarrow H_2$	(5)	= -0.41
CO_2 radical formation		
$CO_2 + e^- \rightarrow CO_2^{\bullet-}$	(6)	= -1.90
Formic acid formation		
$CO_2 + 2H^+ + 2e^- \rightarrow HCO_2H$	(7)	= -0.61
Carbon monoxide formation		
$CO_2 + 2H^+ + 2e^- \rightarrow CO + H_2O$	(8)	= -0.53
Formaldehyde formation		
$CO_2 + 4H^+ + 4e^- \rightarrow HCHO + H_2O$	(9)	= -0.48
Methanol formation		
$CO_2 + 6H^+ + 6e^- \rightarrow CH_3OH + H_2O$	(10)	= -0.38
Methane formation		
$CO_2 + 8H^+ + 8e^- \rightarrow CH_4 + 2H_2O$	(11)	= -0.24
Ethanol formation		
$2CO_2 + 12H^+ + 12e^- \rightarrow C_2H_5OH + 3H_2O$	(12)	= -0.16

Scheme 1. Possible CO_2 photoreduction reaction pathways with reduction potentials.

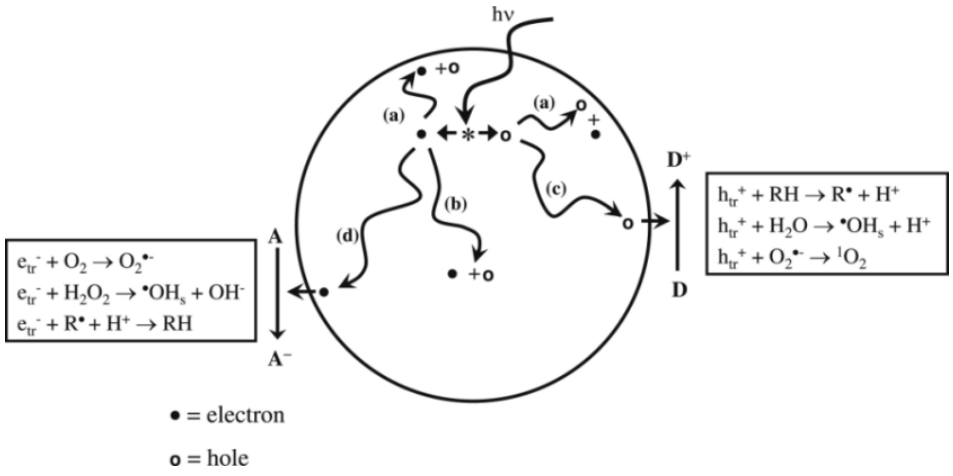

Fig. 2. Charge transfer processes in TiO_2 after UV excitation (Reprinted with permission from Fujishima *et al.*, 2008; Copyright 2008 Elsevier).

for photoreduction. However, as indicated in Scheme 1, in addition to the desired reactions, there are also several competing reactions, such as the formation of H_2 and H_2O_2, which consume H^+ and e^-, respectively (Eqs. (4) and (5)). Research on minimizing the competing reactions is still going on. For example, some researchers have attempted to replace water with other reductants, such as methanol and ethanol (Liu *et al.*, 1998). This provides a high reaction yield and high selectivity to desired products by changing the mechanism. However, water in practice remains the primary reactant since it is readily available and inexpensive.

As for photoreduction reaction pathways, some researchers proposed that CO_2 activation involves the formation of a negatively charged $CO_2^{\bullet-}$ species, which are 23 electron radical anions (Yahaya *et al.*, 2004) and can be detected via infrared (IR) spectroscopy (Hartman and Hisatsune 1966) and electron paramagnetic resonance (EPR) spectroscopy (Perissinotti *et al.*, 2001). However, the single electron transfer to CO_2 occurs at potentials as negative as –1.9 V (Eq. (6)), which is highly endothermic because of the negative adiabatic electron affinity of CO_2 (Lehn and Ziessel, 1982; Freund and Roberts 1996; Indrakanti *et al.*, 2009). The activation of CO_2 molecules in both gas and liquid phases and the formation of $CO_2^{\bullet-}$ are still open questions. Many

researchers now agree that this pathway is a multi-electron transfer (MET) process rather than a single electron transfer process; for the later, the electrochemical potential of –1.90 V precludes the likelihood of a single electron transport mechanism (Lehn and Ziessel, 1982; Yahaya *et al.*, 2004).

As shown in Scheme 1, various products could be formed based on MET photoreduction reactions (Eqs. (7)–(12)). Carbon monoxide (CO) is the most common product, since the reaction needs only two protons and two electrons. Formic acid (HCOOH) is also a common product found in the CO_2 photoreduction system, which consumes the same amount of protons and electrons, but requires slightly higher reduction potential than that for CO formation. The other products are generally difficult to form in gas-solid systems since they need more electrons and protons even though the reactions are thermodynamically favorable. It should be noted that the MET reactions listed in Scheme 1 are just the simplest examples. Some products may be formed through multiple reactions. For example, methane (CH_4) could be formed through Eq. (11) or through the following reactions as well (Varghese *et al.*, 2009; Roy *et al.*, 2010).

$$CO + 6H^+ + 6e^- \rightarrow CH_4 + H_2O \quad (13)$$

$$CH_3OH + 2H^+ + 2e^- \rightarrow CH_4 + H_2O \quad (14)$$

In addition to these desired redox reactions, some backward reactions are also possible, making the CO_2 photoreduction system even more complex. For example, the strong oxidation power of the photoexcited holes, protons, OH radicals, or O_2 could oxidize the intermediates and products to form CO_2.

Limiting Steps and Strategies for Enhancement

The kinetics of CO_2 photoreduction are dependent on many factors, such as reaction temperature, reactant adsorption, product desorption, CO_2 activation, incident light intensity, fraction of the incident light absorbed by the photocatalyst, the specific area of the photocatalyst absorbing the light, and surface as well as crystalline properties of the photocatalysts. For example, CO_2 adsorption on the photocatalyst surface is always considered as a very critical step for CO_2 photoreduction, which could be a pseudo-first-order reaction since the CO_2 photoreduction rate was found to increase with initial CO_2 concentration (Lo *et al.*, 2007). The activation of CO_2 or the electron transfer from the activated photocatalyst to CO_2 is also a major limiting step, where the mechanisms are rather complex and still debatable (Indrakanti *et al.*, 2009). In addition, the e^--h^+ recombination is also widely considered as a major limiting step, which draws mounting attention. Slowing down the e^--h^+ recombination rates has become a key area of research to develop efficient photocatalyst systems. To address the above issues, in particular, to slow down the e^--h^+ recombination rates, several strategies have been developed to enhance the photoreduction efficiency, which are provided as follows.

The first is choosing semiconductors with appropriate bandgap energies/edges. The proper structure of the photocatalyst can improve the product selectivity and yield and increase the rate of reaction. Therefore, photocatalyst preparation is one of the most important steps that can enhance the capacity of a photoreduction system. Wide bandgap semiconductors are the most suitable photocatalysts for CO_2 photoreduction, because they provide sufficient negative and positive redox potentials in conduction bands and valence bands, respectively. The disadvantage of using wide bandgap semiconductors is the requirement for high energy input. Semiconductors with narrow bandgaps, like cadmium sulfide (CdS, 2.4 eV) work in the visible range, but it is not sufficiently positive to act as an acceptor. This causes the photocatalyst to decompose with the hole formation. Table 1 lists several semiconductors with detailed information on their bandgap and band edges.

The second common method is surface modifications of the photocatalysts. For example, one way is to coat metal particles/islands on the semiconductor surface (Fig. 3, left). These metal islands serve as electron sinks to separate e^--h^+ pairs and increase their lifetime (Linsebigler *et al.*, 1995). Formation of composites of two or more semiconductors is also an interesting way. As shown in Fig. 3 (right), in a coupled CdS-TiO_2 system, due to the different band edges of two components, electrons generated from CdS conduction band can transfer to TiO_2 conduction band easily, which increases the charge separation and efficiency of the photocatalytic process (Linsebigler *et al.*, 1995). Doping with non-metals, such as nitrogen is also a promising way to extend the absorption range of the wideband semiconductors from UV to visible range (Sathish *et al.*, 2005). More recently, dye-sensitized and/or enzyme-modified semiconductor systems have also been developed to mimic nature and enhance the photoreduction efficiency. Details of these modifications are provided in the following sections.

COMPARISON BETWEEN DIFFERENT SYSTEMS

Biological Systems

In this section, we will start by presenting a comparison of synthetic systems and their potential for CO_2 conversion; the potential of algal systems for photoconversion is discussed first. Many algae species have been thoroughly investigated for their use in production of biofuels. This motivation stems from two premises: firstly, algae require CO_2 to grow, thus removing CO_2 from the atmosphere; secondly, while the algae grow, many species produce oils and other refinable byproducts that can be used as potential biofuel sources (Kumar *et al.*, 2010; Ho *et al.*, 2011). Therefore, by researching ways in which to maximize algae growth using anthropomorphic CO_2 sources, effective enhancement of a natural biological system that uses solar energy to convert CO_2 into potential fuel sources can be achieved. Fig. 4 shows how photosynthesis occurs in algae. In algae, the fixation of CO_2 occurs as a result of two separate reaction steps. In the light-dependent set of reactions, photoexcited electrons are used to reduce the coenzyme $NADP^+$ to NADPH as well as create the high-energy molecule ATP. In the second set of reactions, called the light-independent reactions, these reduced molecules are used to convert CO_2 to organic compounds that can then

Table 1. List of semiconductors with detailed bandgap information (Koffyberg and Benko, 1982; Matsumoto, 1996; de Jongh *et al.*, 1999; Xu and Schoonen, 2000; Carlson *et al.*, 2008; Li *et al.*, 2010a; Chikata *et al.*, 2013).

Name	Formula	E_g (eV)	CB Edge (eV) at pH = 7	VB Edge (eV) at pH = 7	λ (nm)	Range
Silicon	Si	1.1	–0.6	0.5	1125	
Tungsten selenide	WSe_2	1.4	–0.25	1.15	1032	IR
Copper (II) oxide	CuO	1.35	4.07	5.42	1032	
Copper (I) oxide	Cu_2O	1.9	–1.30	0.60	620	
Cadmium selenide quantum dots	CdSe QDs	200	1.2	3.2	620	
Ferric oxide (α-phase)/Hematite	α-Fe_2O_3	2.2	0.13	2.33	560	
Bismuth vanadate	$BiVO_4$	2.4	–0.30	2.1	517	
Cadmium sulfide	CdS	2.4	–0.6	1.8	517	
Tungsten oxide	WO_3	2.5–2.8	0	2.5–2.8	495–442	VIS
Indium tantalum oxide	$InTaO_4$	2.6	–0.75	1.85	477	
Vanadium pentoxide	V_2O_5	2.7	–4.7 (pH 6.54)	–2.0	458	
Indium oxide	In_2O_3	2.9	–3.88 (pH 8.64)	–0.98	428	
Silicon carbide	SiC	3.0	–1.5	1.5	415	
Titanium oxide (Rutile)	TiO_2	3.02	–0.52	2.5	410	
Titanium oxide (anatase)	TiO_2	3.23	–0.29	2.94	384	
Zinc oxide	ZnO	3.2	–0.31	2.91	387	
Strontium titanate	$SrTiO_3$	3.4	–3.24 (pH 8.6)	0.16	364	
Tin dioxide	SnO_2	3.5	–4.5 (pH 4.3)	–1.0	354	
Manganese (II) oxide	MnO	3.6	–3.49 (pH 8.61)	0.11	345	UV
Zinc sulfide	ZnS	3.7	–3.46 (pH 1.7)	0.24	335	
Nickel oxide	NiO	4.3	–0.5	4.8	288	
Aluminum oxide	Al_2O_3	7.1	–3.6	3.5	175	
Magnesium oxide	MgO	7.3	–3.0	4.3	159	

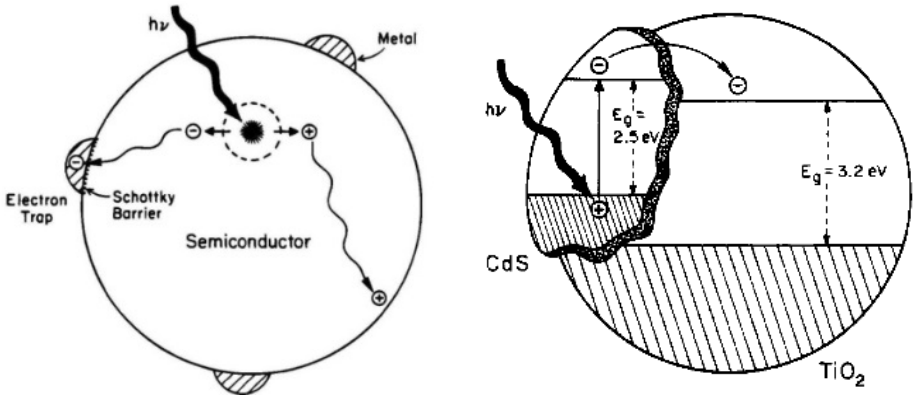

Fig. 3. Schematic diagram of metal-doped semiconductors for electron-hole separation (left) and composite semiconductor systems (right) (Reprinted with permission from Linsebigler *et al.*, 1995; Copyright 1995 American Chemical Society).

be used by algae as a source of energy. The oils produced by algae which are used for biofuel production contain the carbon that was fixed in the Calvin cycle. It can be seen that this biological system is similar in function to synthetic systems, with the added step of electron transfer to ADP and $NADP^+$ to form high energy molecules for subsequent reduction to occur in the Calvin cycle (Zeng *et al.*, 2011).

In a synthetic system, light energy is used to excite electrons in the photocatalyst which are then used to reduce CO_2. Thus, light energy is stored in the bonds of the reduced CO_2 products. It is apparent that the steps carried out in these synthetic systems very much resemble what is accomplished with algae. Tables 2 and 3 summarize different species of algae and synthetic systems with their CO_2 conversion rates, respectively. In order to make a fair comparison between these systems it is important to use one consistent unit of measurement for CO_2 conversion, such as μmol CO_2 converted per gram catalyst per hour (μmol/g/h). Out of the many ways CO_2 conversion is reported in the literature for synthetic systems, this unit seems to the best to demonstrate the performance of the system, as it truly reflects the potential of conversion of the system without bias of amount of catalyst used or amount of time used to run the experiment. For algae systems, a commonly reported unit in the literature is mg of CO_2 consumed per liter of culture fluid per day (mg/L/d). For

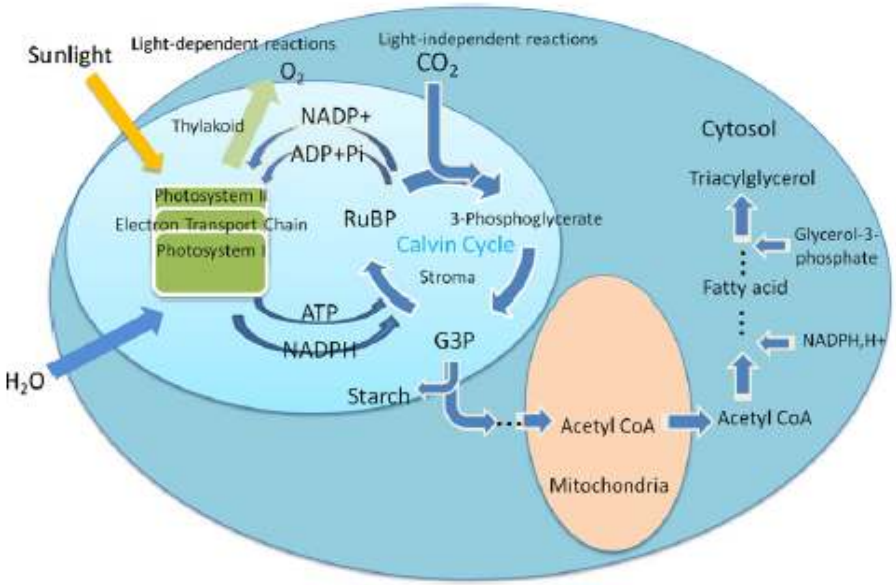

Fig. 4. Schematics of photosynthesis - CO_2 fixation and carbon accumulation in microalgae cells (Reprinted with permission from Zeng *et al.*, 2011; Copyright 2011 Elsevier).

Table 2. Summary of algae systems for CO_2 fixation and conversion.

Algae Species	Conversion (μmol/g/h)	References
Nannochloris Sp.	57–569	(Negoro *et al.*, 1991)
Nannochloroposis sp.	48–481	(Negoro *et al.*, 1991)
Phaeodactylum tricornutum	27–267	(Negoro *et al.*, 1991)
Chlorella sp.	125–1246	(Sakai *et al.*, 1995)
Chlorococcum LIttorale	85–852	(Kurano *et al.*, 1995)
Synechocystis	142–1420	(Murakami and Ikenouchi, 1997)
Botryococcus braunii	95–947	(Murakami and Ikenouchi, 1997)
Chlorella sp.	167–1673	(Sung *et al.*, 1999)
Chlorella vulgaris	7–71	(Scragg *et al.*, 2002)
Chlorella emersonii	7–73	(Scragg *et al.*, 2002)
Scenedesmus sp	44–436	(Jin *et al.*, 2006)
Chlorella vulgaris	58–580	(Jin *et al.*, 2006)
Microcystis aeruginosa	49–493	(Jin *et al.*, 2006)
Microcystis ichthyoblabe	46–464	(Jin *et al.*, 2006)
Chlorella vulgaris	591–5909	(Cheng *et al.*, 2006)
Euglena gracilis	36–362	(Chae *et al.*, 2006)
Chlorella kessleri	16–155	(de Morais and Costa, 2007c)
Scenedesmus obliquus	15–152	(de Morais and Costa, 2007c)
Spirulina sp.	36–358	(de Morais and Costa, 2007a)
Scenedesmus obliquus	25–259	(de Morais and Costa, 2007a)
Spirulina sp.	37–373	(de Morais and Costa, 2007b)
Scenedesmus obliquus	19–188	(de Morais and Costa, 2007b)
Chlorella kessleri	12–116	(de Morais and Costa, 2007b)
Chlorella vulgaris	335–3352	(Fan *et al.*, 2008)
Chlorella sp	81–812	(Chiu *et al.*, 2008)
Chlorella sp	68–680	(Chiu *et al.*, 2009)
Chlorella sp	109–1086	(Chiu *et al.*, 2009)
Chlorella sp	66–663	(Ryu *et al.*, 2009)
Aphanothece microscopica Nageli	136–1364	(Jacob-Lopes *et al.*, 2009b)
Aphanothece microscopica Nageli	515–5147	(Jacob-Lopes *et al.*, 2009a)
Anabaena sp.	137–1373	(Lopez *et al.*, 2009)
Scenedesmus sp.	39–387	(Yoo *et al.*, 2010)
Scenedesmus obliquus	52–521	(Ho *et al.*, 2010)

Table 3. Literature summary of CO_2 photoreduction by semiconductors, metal-organic, and hybrid systems.

Catalysts	Product (s)	Conversion (μmol/g/)	Reference
Semiconductor Systems			
Pt NP/TiO_2 film	CH_4	1361	(Wang *et al.*, 2012b)
TNTs- Bi_2S_3	CH_3OH	224.6	(Li *et al.*, 2012b)
TNTs-CdS	CH_3OH	159.5	(Li *et al.*, 2012b)
Cu/TiO_2/SiO_2 (wet method)	CO	45	(Li *et al.*, 2010b)
Cu/TiO_2/SiO_2 (aerosol method)	CO	20	(Wang *et al.*, 2011c)
PbS QD/Cu-TiO_2	CO	1.71	(Wang *et al.*, 2011b)
TiO_2/GO layered sheets	CO/CH_4	10.0	(Tu *et al.*, 2012)
Pt loaded c-$NaNbO_3$	CH_4	4.86	(Li *et al.*, 2012a)
CdS-MMT	CH_4/CO/H_2	8.4	(Praus *et al.*, 2011)
Anatase(75%) Brookite (25%)	CO	2.1	(Zhao *et al.*, 2013)
TiO_2-RMA	CH_4	2.4	(Wang *et al.*, 2012a)
Cu/Fe-TiO_2-SiO_2	CH_3OH	4.12	(Wu, 2009)
Ti-Sillica Film	CH_4 CH_3OH	11	(Jacob-Lopes *et al.*, 2009a)
MgO	CO	4	(Kohno *et al.*, 2001)
ZrO_2	CO	5	(Kohno *et al.*, 2000)
Ti-MCM-41 and 48	CH_4/CH_3OH	10.5	(Anpo *et al.*, 1998)
TiO_2 (Degussa P-25)	CH_4/CH_3OH	93.8	(Ku *et al.*, 2004)
Cu-TiO_2 dye sensitized	CH_4	0.3	(Yuan *et al.*, 2012)
Nafion layer on Pd-TiO_2	CH_4/C_2H_6	3.3	(Kim *et al.*, 2012)
MWCNT-TiO_2 (anatase, rutile)	CH_4/HCO_2H	73.33	(Xia *et al.*, 2007)
CoPc-TiO_2	HCOOH/CH_4	33.5	(Liu *et al.*, 2007)
Cu-TiO_2	CH_3OH	20	(Tseng *et al.*, 2004)
Cu-TiO_2	CH_3OH	12.5	(Tseng *et al.*, 2002)
Ti-Silica porous thin film	CH_4/CH_3OH	9.1	(Ikeue *et al.*, 2002)
TiO_2 powder	HCOOH	1.8	(Kaneco *et al.*, 1999)
Rh-TiO_2	CO/CH_4	5.2	(Kohno *et al.*, 1999)
TiO_2/zeolite	CH_3OH	13	(Yamashita *et al.*, 1998)
TiO_2 (P-25)	CH_4	0.43	(Kaneco *et al.*, 1998)
CdS coated by thiol TiO_2 (P-25)	Formate, CO	96.1	(Liu *et al.*, 1998)
TiO_2/zeolite	CH_4	13.3	(Anpo *et al.*, 1997)
Biohybrid Systems			
TiO_2/CODH I/Ru dye	CO	250	(Woolerton *et al.*, 2010)
CdS QD/CODH I	CO	60	(Chaudhary *et al.*, 2012)
TiO_2/malic enzyme	Malic acid	1107	(Inoue *et al.*, 1992)
TiO_2/Formate dehydrogenase	HCOOH	0.01	(de Morais and Costa, 2007a)
Enzyme/Graphene complex	HCOOH	110000	(Yadav *et al.*, 2012)
Metal-Organic Complex Systems			
[Re(bpy)$(CO)_3$Cl]	CO	30 TON[a]	(Chauvin *et al.*, 2011)
Ru(II)/Re(I) dimers	CO	90 TON	(Bian *et al.*, 2012)
Rhenium complex	CO	30 TON	(Takeda *et al.*, 2008)
Metalorganic-polyoxometalate hybrid complex	CO/CH_4	23.6 TON	(Ettedgui *et al.*, 2011)
Ru-substituted polyoxometalate	CO	3 TON	(Khenkin *et al.*, 2010)
[Re(I)$(CO)_3$(dcbpy)Cl](H_2L_4) derivatized MOF4	CO	10.9 TON	(Wang *et al.*, 2011a)
$Co(bpy)_3^{2+}$ with $Ru(bpy)_3^{2+}$	H_2/CO	8.3 TON	(Hirose *et al.*, 2003)
[*fac*-Re(bpy)-$(CO)_3P(O^iPr)_3]^+$	CO/H_2	15.6 TON	(Hori *et al.*, 2002)

[a] (TON = turnover number) results for organic complex systems are reported in turnover numbers because of lack of information for conversion to the metric μmol/g/h. The turnover number is the maximum number of substrate molecules that the molecular catalyst can convert to product, per site available on the catalyst (Morris *et al.*, 2009).

instance, Ho *et al.* (2011) reported the CO_2 consumption rate of the algae species in Table 2 in the unit mg/L/d. We converted this unit to μmol/g/h for comparison with synthetic systems. This unit conversion was accomplished by assuming 1 gram of dry algae in the culture fluid, which is a typical range of dry algae reported for 1 liter of culture fluid.

As we can see from the two tables, in general, synthetic systems conversion rates fall below the algal systems. However, it should be noted that in order to produce well performing algae systems a lot of resources must be

consumed. The tanks for the algae must be cleaned frequently in order to prevent such as water and nutrients buildup that blocks light penetration. As mentioned earlier, for just one gram of algae up to an entire liter of water is required. Therefore, a lot of space and water resources are required to get the performance as outlined in the table above. The CO_2 uptake occurs in the algal biomass that requires cumbersome separation steps for the extraction of the oil product. Furthermore, algae systems are in general less robust in stability compared to synthetic systems. Algae are living organisms that require a narrow range of living conditions, thus small changes in their environment can impact biomass growth as well as the amount of byproducts produced, for which a lot of time and energy is required in process control to guarantee optimal performance. Very few, if any, synthesis have demonstrated uptake of CO_2 from concentrated systems exceeding a few percent. Synthetic systems however, do not have these growth associated problems of a biological system. While it is true that current synthetic systems have decreased activity after a certain amount of time leading to a decrease in conversion rates, there is a lot of room to improve and modify these systems; whereas most of the problems associated with algae systems are due to algae being a living organism, which makes the problem for improvement comparatively more complicated. Thus it is important to not only improve the conversion rates of synthetic systems but also to improve the lifetime of these systems for practical and scalable use in the future.

Semiconductor Systems

There are many types of synthetic systems covered in the literature. The most common and thoroughly researched synthetic systems are semiconducting materials, such as TiO_2.

TiO_2-Related Photocatalysts

TiO_2 is a commonly used wide bandgap semiconductor for CO_2 photoreduction because of its relatively low cost, high availability, resistance to photo-induced corrosion and low toxicity (Indrakanti *et al.*, 2009).

TiO_2 Nanomaterials. The first CO_2 photoreduction system involved the use of semiconductor powders such as TiO_2 suspended in a beaker of water (Inoue *et al.*, 1979). Improvements have been made to these systems with the advent of semiconductor nanoparticles (NPs) which led to an increase in the surface area of a semiconductor catalyst. By using TiO_2 NPs, the catalytically active surface area is increased, leading to an increase in the frequency between CO_2 and TiO_2, a crucial factor for the electron transfer in reductive reactions in Scheme 1, as well as to leading to a decreased amount of e^--h^+ recombination that occurs on the TiO_2 surface. P25 is a commercially available source of anatase-rutile mixed phase TiO_2 NPs that is commonly purchased and employed in photocatalytic research. Its popularity stems from its high catalytic activity that arises from the repressed recombination rates that is a result of the ratios of mixed anatase and rutile phases employed in the P25 formulation (Hurum *et al.*, 2003).

TiO_2 crystal structure and morphology studies are commonly explored in the literature as methods for increasing TiO_2 photocatalytic activity. TiO_2 nanosheets with 95% exposed {100} facet are a good example to demonstrate the crystal structure effect. Marked photocatalytic activity was achieved since the {100} facet was considered to be the active facet (Xu *et al.*, 2013). By changing the morphology of TiO_2, the electron transport through the TiO_2 could be controlled. The most studied morphology is the porous arrays or spheres. For instance, porous microspheres of MgO-patched TiO_2 were synthesized by Liu *et al.* (2013). The microspheres exhibited 10 times higher activity toward CO production when the reaction temperature increased from 50 to 150°C. However, this morphology also suffers from having multiple grain boundaries that cause erratic electron transport through the network leading to undesired electron recombination. By changing to a patterned film structure or nanowire/rod configuration, the electron transport can be oriented to be more direct in one path so that electron recombination between two individual TiO_2 structures is minimized. For example, the synthesis and characterization of anatase phase nanorods modified with rutile phase NPs (TiO_2-RMA) for the photoreduction of CO_2 were reported (Wang *et al.*, 2012a).

The rutile phase NPs served as an electron sink in place of more commonly used and more expensive Pt NPs. Wang *et al.* (2012a) showed that this TiO_2-RMA structure showed greater conversion rates than just anatase phase nanorods. While the transition from semiconductor powders to semiconductor NPs has effectively increased the surface area of TiO_2 catalytic systems, additional modifications to TiO_2 are required to enhance activity that is a result of its wide band-gap, which restricts excitation to the UV range, which constitutes only 3–5% of the solar spectrum. Furthermore, modifications to reduce e^--h^+ recombination rates and increase CO_2 availability at the catalyst surface must be made to see the upper-level efficiencies possible for TiO_2 systems.

Modifications of TiO_2 Systems. Common modifications made to TiO_2 include doping of the TiO_2 lattice with metal and nonmetals, leading to reduced e^--h^+ recombination rates and visible sensitivity, respectively. The formation of heterojunctions by incorporating two or more components (metals or semiconductors) with different energy levels is another effective approach for this purpose. Catalytically inactive supports such as SiO_2 are used to physically separate TiO_2 NPs while effectively increasing surface area. Crystal phase modification is also an interesting topic to explore.

By doping metals such as Cu, Pt, Fe in the TiO_2 lattice or coating the metals/metal oxides onto the TiO_2 surface, it has been found that the conversion rates of the photocatalytic reduction for these systems are higher than their non-modified counterparts. In the case of doping or coating metals, this can be explained by considering the metal dopants/islands as sinks for the excited TiO_2 electrons (Usubharatana *et al.*, 2006). When the excited electron is injected into the conduction band of the TiO_2 and starts to travel across the TiO_2 crystal lattice, it becomes trapped by the metal dopants because of the relative lower energy state that it can obtain if it goes to the metal dopant. Thus the metal

dopant/island serves as a means in which to separate the excited electrons from the holes that are in the TiO_2 lattice, thereby reducing e^--h^+ recombination. For heterojunctions with mixed semiconductors, the difference between band-edges is the major driving force for the enhancement of charge transfer and subsequently the photocatalytic performance. As from Fig. 5, upon deposition of Cu species (Cu_2O in this case) on the TiO_2 surface not only did the amount of CO_2 reduced and thus product yielded increase, but also formed a new product, CH_4. The formation of *pn* junction between Cu_2O and TiO_2 is considered as the major reason for the improvement.

Electron sinks that are noble metals, such as Pt and Rh, also have implications in multi-electron transfer reactions that are crucial for high efficiency photocatalytic reduction of CO_2 to take place (Indrakanti *et al.*, 2009). It has also been found that the size of the noble metal NP used to serve as the electron sink is a crucial variable in the conversion rates that can be achieved. Wang *et al.* (2012b) reported a facile synthesis for Pt-TiO_2 nanostructured films using an aerosol chemical vapor deposition route (ACVD) to deposit the TiO_2 film and a tilted-target sputtering (TTS) technique to deposit Pt NPs. It was observed that if the Pt NP is too small, then quantum confinement effects cause the energy band separation of the Pt NP to be too high for an excited electron to be transferred to the NP. Conversely, if the Pt NP is too big, the NP merely serves as a recombination center capturing both excited electrons and holes, vastly reducing the efficiency of the system (Wang *et al.*, 2012b). Thus precise control over the size of the metal dopant plays a role in the CO_2 conversion rates for the system. Fig. 6 provides a graphic description of the photocatalytic steps in this system along with the change in energy levels of the Pt NPs as a function of their size. Doping of Au or Ag can also extend the sensitivity of the photocatalyst to the visible spectrum due to their localized surface plasmonic resonance properties (Li *et al.*, 2007).

Nonmetal doping has also been used for TiO_2 photocatalytic reduction systems. However the function desired from nonmetal doping is much different from that of metal doping. The doping of nonmetals such as nitrogen or carbon is motivated by trying to extend the electromagnetic region in which the photocatalyst is able to use to generate excited electrons by narrowing the bandgap of the photocatalyst system (Hamadanian *et al.*, 2009). The nonmetal dopants effectively redshift the TiO_2 photocatalyst

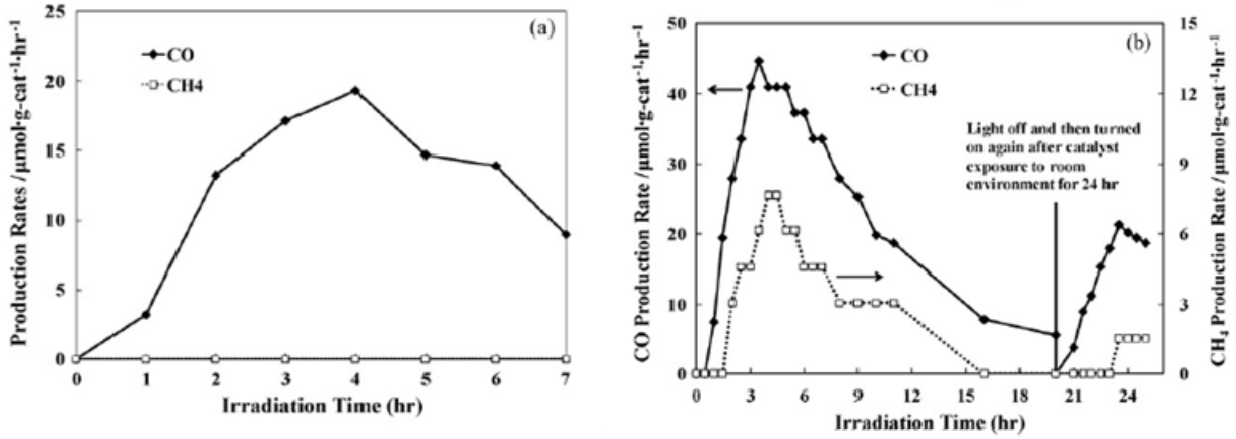

Fig. 5. Production rates of CO and CH_4 as a function of irradiation time for (a) TiO_2-SiO_2 and (b) 0.5% Cu_2O modified TiO_2-SiO_2 (Reprinted with permission from Li *et al.*, 2010b; Copyright 2010 Elevier).

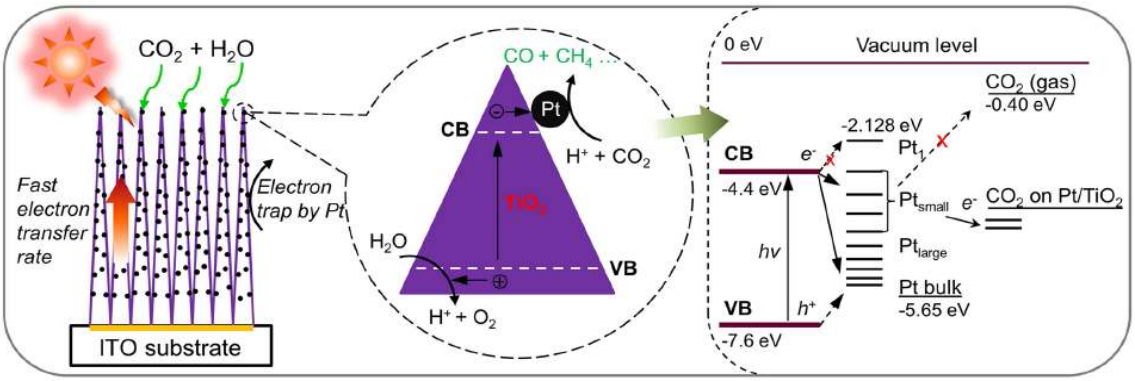

Fig. 6. Schematic of CO_2 photoreduction on Pt modified TiO_2 thin films with highly directed electron flow. On the right is provided a bandgap description of the effect of Pt size on CO_2 photoreduction (Reprinted with permission from Wang *et al.*, 2012b; Copyright 2012 American Chemical Society).

system thus allowing for a greater portion of the incoming light's spectrum to be used for generating e^--h^+ pairs (Yu *et al.*, 2002). Sathish *et al.* (2005) also reported higher photocatalytic activity for a N-TiO_2 system. The photocatalytic activity of the N-TiO_2 system exposed to visible light was reported to be higher than pure TiO_2 and P25. The shift from UV only to visible sensitization is shown clearly in Fig. 7.

TiO_2 Crystal Structure. TiO_2 exists in three distinct crystal forms called rutile, anatase and brookite. Of these crystal phases, rutile and anatase are the best understood and studied. There is much research being conducted on exploring the effect of TiO_2 crystal structure on photocatalytic activity. Pan *et al.* (2011) reported a synthesis technique for faceted anatase rods. These faceted rods showed higher photocatalytic conversion of CO_2 to CH_4 when loaded with Pt NPs than P25 loaded with Pt did, thus showing how significant a simple change to crystal structure can greatly affect and improve a photocatalytic system.

Out of the three phases, brookite is the least studied and the optimum composition for an anatase-brookite photocatalyst for the reduction of CO_2 has only been explored once in the literature to date (Liu *et al.*, 2012; Zhao *et al.*, 2013), while rutile-anatase systems are more common and can be purchased in the form of P25. Zhao *et al.* (2013) has reported an optimal composition of anatase-brookite systems as 75% anatase and 25% brookite. This optimized system showed higher photocatalytic activity than P25, which suggests that the interaction leading to greater photocatalytic activity for the rutile/anatase combination for P25 compared to anatase and rutile alone is not as effective as the interaction between anatase and brookite. It is interesting to note that the composition, 75% anatase and 25% brookite that was found to be optimal is the same fractions used for many commercially available anatase-rutile P25, further supporting the idea that the anatase-brookite interaction is more favorable than the anatase-rutile interaction for enhanced photocatalytic activity.

TiO_2 in Mesoporous Supports. By incorporating SiO_2 as a mesoporous support into the TiO_2 lattice it has been found that the photocatalytic activity of the system increases (Anpo *et al.*, 1986, 1998). While the SiO_2 in the system is not photocatalytically active, it is understood that the SiO_2 mesoporous network serves to not only spatially separate the TiO_2 NPs but also serves to increase the surface area of the system for CO_2 to bind and be reduced. Furthermore, the dispersion of TiO_2 NPs into the SiO_2 network reduces contact between the TiO_2 NPs leading to less e^--h^+ recombination occurring between individual particles (Wang *et al.*, 2011c).

Wang *et al.* (2011c) reported a low cost, rapid synthesis technique using a furnace aerosol reactor (FuAR) for the synthesis of Cu-TiO_2-SiO_2 photocatalyst composite particles formed by evaporation driven self-assembly. The size, composition, and porosity of the composite particle were controlled by adjusting the temperature of the reactor, the precursor concentrations and the ratio of each constituent present in the feed to the FuAR. Fig. 8 shows a schematic of the experimental setup for catalysis synthesis and analysis. It was reported that a relatively high conversation rate of 20 μmol/g/h of CO was obtained, showing the high potential for aerosol pathways for the synthesis of photocatalysts compared to more time consuming wet chemical based techniques. The synergistic effect of deposition with Cu_2O and dispersing the TiO_2 NPs in a silica mesoporous matrix has been reported in the literature and it was found that the photocatalytic conversion rates and selectivity for CH_4 was increased (Fig. 5, Li *et al.*, 2010b).

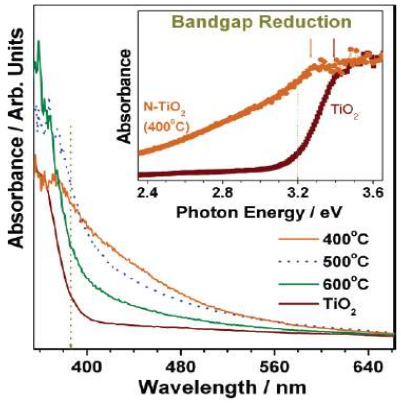

Fig. 7. UV-vis absorption spectrum of N-TiO_2 at varying calcination temperatures (Reprinted with permission from Sathish *et al.*, 2005; Copyright 2005 American Chemical Society).

Other Semiconductors

Current photocatalytic systems for the reduction of CO_2 are not limited to just TiO_2. There are many other semiconductor-based systems reported in the literature. Some of these semiconductors include CdS, ZnO, GaP, SiC, WO_3, and various other metal oxides. One of the possible advantages of using non TiO_2 semiconductors is a narrower bandgap that results in a wider range of wavelengths to induce excitation of electrons (Navalon *et al.*, 2013). This has implications in visible light range sensitivity without the use of sensitizers that are subject to photo-degradation, thus allowing for a possible more stable system under visible light conditions. Praus *et al.* (2011) reported the synthesis of CdS NPs deposited on montmorillonite (MMT) and found that the photocatalytic activity of the resulting CdS-MMT nanocomposite was 4-8 times greater than P25.

Cao *et al.* (2011) reported the use of carbon NPs covalenty functionalized with gold and platinum to concentrate the photogenerated electrons for the ultimate reduction of CO_2. This functionalization gives carbon NPs strong absorption in the visible range and possible near-IR range as well. It was reported that when tested for its photocatalytic activity, formic acid was found to be the main product with a quantum yield of ~0.3% which was said to be an order of magnitude higher than what was obtained for TiO_2 using similar experimental conditions except with exclusion of the visible range. It can be seen that research surrounding these alternative semiconductor systems that naturally absorb greater in the visible region is relative, as their photocatalytic capabilities in comparison to more traditional TiO_2 systems are promising.

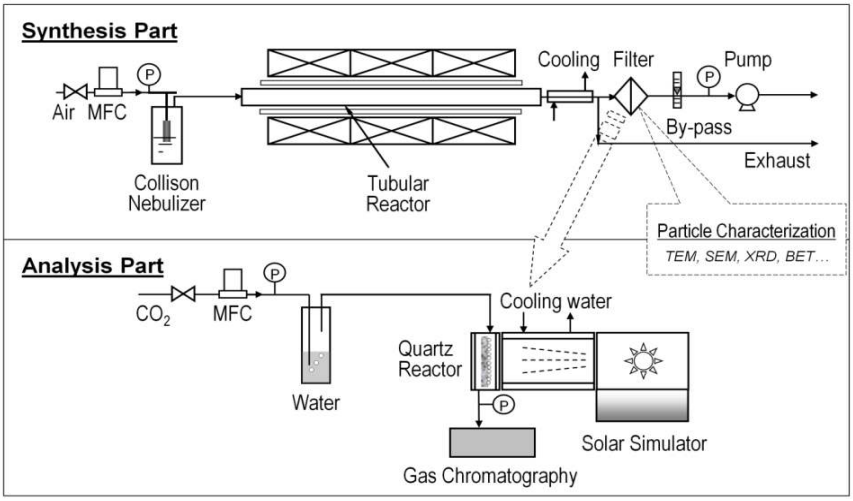

Fig. 8. Experimental setup for aerosol processing of catalysts and CO_2 photoreduction analysis (Reprinted with permission from Wang *et al.*, 2011c; Copyright 2011 Royal Society of Chemistry).

Metal sulfide systems have also been paired with titania-based systems to sensitize for visible light. Li *et al.* (2012b) reported the use of TiO_2 nanotubes (TNTs) with Bi_2S_3 and CdS modification that led to both increased visible light absorption and catalytic activity of the TNTs. As from Table 3, these values are rather high showing promise for systems that incorporate non titania based semiconductors.

Metal-Organic Complex Systems

CO_2 reduction systems employing large molecular compounds can be divided into two types. The first type of system is characterized by the electron excitation and catalytic reduction of CO_2 taking place at two different sites, while the second type of system involves the excitation and catalytic reduction taking place on the same large molecular complex (Morris *et al.*, 2009). The first system can be thought of as a photo-sensitized system, which commonly uses Ru-dyes for the sensitization. These types of systems have been discussed previously in this study, however were not specifically classified until now as the use of dye sensitizers in semiconductor systems to extend sensitization of the semiconductor catalyst into the visible range is so ubiquitous in the literature. For this review, we will focus mostly on type two systems in which the sensitizer and catalyst of the system are the same large molecule and type one systems in which the catalyst is not a metal semiconductor, but rather another molecular complex covalently bonded to the sensitizer.

Bruckmeier *et al.* (2012) reported the photocatalytic activities of type 2 rhenium(I) based catalysts, which stated that the transfer of the second electron for CO_2 reduction to CO originates from the long lived one-electron reduced species (OER), dominates if the proximity of the coordination centers is adjusted according to the lifetime of the OER. In the case of Re-NCS type complexes with a naturally long lived OER, the bimetallic mechanism will occur by simply increasing the concentration of the catalyst, which changes the proximity of the coordination centers, thus it has often been the case in the literature that Re-NCS photocatalysts are reported as the best rhenium(I) based photocatalysts. However, Bruckmeier *et al.* (2012) reported that in fact Re-Br photocatalysts showed better photocatalytic activity if the centers are brought in closer proximity through covalent linkage, which would be expected considering the ease with which the bromo-ligand leaves thus providing a new coordination site.

Ettedgui *et al.* (2011) reported the synthesis of a metalorganic polyoxometalate hybrid complex, $Re^{I}(L)(CO_3)CH_3CN$-$MHPW_{12}O_{40}$ (L = 15-crown-5-phenanthroline and M = Na^+, H_3O^+), for the photoreduction of CO_2 in visible light. This system showed high conversion rates and the structure of this complex is provided in Fig. 9. Chauvin *et al.* (2011) reported the use of type 2 osmium complexes for the photoreduction of CO_2 in visible light with the use of an amine sacrificial agent. It was reported that conversion rates were comparable to rhenium based systems thus making osmium complexes a possible alternative.

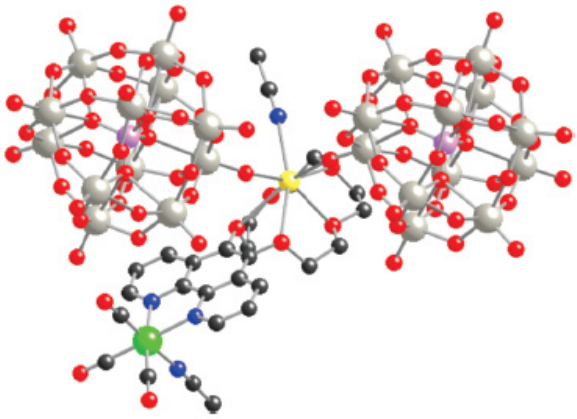

Fig. 9. Ball and stick structure of metalorganic polyoxometalate hybrid complex, $Re^{I}(L)(CO_3)CH_3CN$-$MHPW_{12}O_{40}$ (L = 5-crown-5-phenanthroline and M = Na^+, H_3O^+). C, black; N, blue; O, red; P, purple; Na, yellow; Re, green; W, gray (Reprinted with permission from Ettedgui *et al.*, 2011; Copyright 2011 American Chemical Society).

These systems have the advantage of not requiring the use of expensive co-catalyst metals such as Pt, Au. Furthermore, the amount of modifications and changes that can be made to the structure of the molecules involved in each system provides a lot of variables for experimentation and improvement of this type of photocatalytic system. However, a problem worth noting is that many of these systems suffer from photo-degradation that ruins the catalytic behavior of the dye shortly after exposure to a light source. Furthermore, many of these systems require a sacrificial agent for restoration of the depleted sensitizer, which is not desired in the long term for CO_2 photoreduction systems. There is much literature regarding the synthesis of novel molecular complexes for the photocatalytic reduction of CO_2. However, it is interesting to compare these types of systems with their parallel in biology. In biology, large molecular complexes called proteins are responsible for both electron transport, that results from excitation upon incidental visible light, as well as for the conversion of CO_2 in plants. We will now provide a discussion of some of these bio-inspired systems that use enzymes for the catalyzed CO_2 conversion step on a semiconducting material.

Hybrid Systems

A more trendy area of research for CO_2 photoreduction includes incorporating enzymes to carry out the catalytic step. The goal behind using enzymes is to set a benchmark of what synthetic systems should be capable, based on the fact that enzymes have evolved to perform the catalytic step with high efficiency (Woolerton *et al.*, 2012). Enzymes are highly substrate specific, show high rates of conversion, and have evolved to be highly efficient at carrying out their catalytic functions. Thus they are an attractive option for proof- of-concept CO_2 photoreduction systems.

As early as 1992, Inoue *et al.* (1992) used malic enzymes isolated from chicken liver to carry out the catalytic reduction of CO_2. The enzymes were paired with both TiO_2 microcrystals and CdS particle suspension systems and showed conversion of pyruvic acid to malic acid. Woolerton *et al.* (2012) conducted similar experiments using a carbon monoxide dehydrogenase (CODH) enzyme. Their basic system involved the CODH enzyme and a Ru-based dye adsorbed onto the surface of TiO_2 NPs. The dye served as a visible light sensitizer and upon excitation injects its electrons into the conduction band of the TiO_2 nanoparticle which then serves to transport the electrons to the enzyme. The enzyme then carries out the catalyzed reduction step. This system showed high selectivity for CO and the conversion rate was reported as 250 μmol/g/h. Below in Fig. 10 is visual representation for this system.

Chaudhary *et al.* (2012) reported co-attching CODH enzyme to both CdS quantum dots (QDs) and CdS nanorod (NR) morphologies. It was reported that while the QD-CdS-CODH system showed a higher conversion rate at 60 μmol/g/h. The NR-CdS-CODH showed a much higher turnover rate at 1.23 s^{-1} compared to 0.25 s^{-1} for the QD-CdS-CODH system. Yadav *et al.* (2012) reported the use of a novel graphene-based visible light active photocatlyst that incorporates a covalently bonded chromophore, such as multianthraquinone substituted porphyrin to the graphene oxide (GO) as a photocatalyst coupled with the activity of the enzyme, formate dehydrogenase. In this system, the chromophore is excited and transports its electrons into the GO. The electrons are then transferred to a rhodium complex in solution which becomes reduced. The reduced rhodium complex then reduces the co-enzyme NAD^+ to NADH which is consumed by the formate dehydrogenase enzyme to carry out the reduction of CO_2 to formic acid, thus completing the catalytic cycle (Yadav *et al.*, 2012). The conversion rate for this system was high, showing not only how enzyme incorporation into a photocatlytic system can provide high efficiency, but also shows the future for systems that incorporate graphene-based materials in CO_2 photoreduction systems.

SUMMARY AND OUTLOOK

Photoreduction of CO_2 is a promising approach to reduce carbon emission while simultaneously recycles it as a fuel feedstock by harnessing readily available solar energy. The reduction mechanisms, however, are complex, involving various limiting steps. Overcoming the limiting steps is the major task for developing efficient photocatalyst systems. Several strategies have been reviewed for this purpose, including selection of semiconductors with suitable band edges, coating electron sinks, forming heterogeneous junctions, designing novel morphologies, and developing hybrid structures. A state-of-the-art comparison between

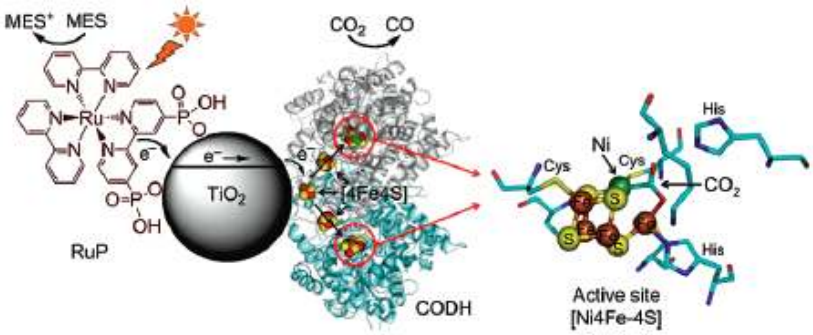

Fig. 10. Schematic of CO_2 photoreduction on *Ch* CODH I modified dye-sensitized TiO_2 NP (Reprinted with permission from Woolerton *et al.*, 2010; Copyright 2010 American Chemical Society).

different photocatalytic systems for CO_2 reduction was made aiming to demonstrate the advances in this area and provide an overview of the research trend for future development of photocatalysts for CO_2 photoreduction in a large scale.

ACKNOWLEDGMENTS

The authors would like to acknowledge the support from the Consortium for Clean Coal Utilization (CCCU) at Washington University in St. Louis. Partial support from the Nano Research Facility (NRF, a member of NSF-NNIN) at Washington University in St. Louis is greatly acknowledged. Partial support from USEPA through Pegasus contract EP-011-006 is acknowledged. Any opinions expressed in this paper are those of the authors and do not necessarily reflect the views of the Agency; therefore, no official endorsement should be inferred.

REFERENCES

Abe, T., Yoshida, T., Tokita, S., Taguchi, F., Imaya, H. and Kaneko, M. (1996). Factors Affecting Selective Electrocatalytic CO_2 Reduction with Cobalt Phthalocyanine Incorporated in a Polyvinylpyridine Membrane Coated on a Graphite Electrode. *J. Electroanal. Chem.* 412: 125–132.

Anpo, M., Nakaya, H., Kodama, S., Kubokawa, Y., Domen, K. and Onishi, T. (1986). Photocatalysis over Binary Metal-Oxides - Enhancement of the Photocatalytic Activity of Tio_2 in Titanium Silicon-Oxides. *J. Phys. Chem.* 90: 1633–1636.

Anpo, M., Yamashita, H., Ichihashi, Y., Fujii, Y. and Honda, M. (1997). Photocatalytic Reduction of CO_2 with H_2O on Titanium Oxides Anchored within Micropores of Zeolites: Effects of the Structure of the Active Sites and the Addition of Pt. *J. Phys. Chem. B* 101: 2632–2636.

Anpo, M., Yamashita, H., Ikeue, K., Fujii, Y., Zhang, S.G., Ichihashi, Y., Park, D.R., Suzuki, Y., Koyano, K. and Tatsumi, T. (1998). Photocatalytic Reduction of CO_2 with H_2O on Ti-MCM-41 and Ti-MCM-48 Mesoporous Zeolite Catalysts. *Catal. Today* 44: 327–332.

Bian, Z.Y., Wang, H., Fu, W.F., Li, L. and Ding, A.Z. (2012). Two Bifunctional Ru-II/Re-I Photocatalysts for CO_2 Reduction: A Spectroscopic, Photocatalytic, and Computational Study. *Polyhedron* 32: 78–85.

Biswas, P., Wang, W.N. and An, W.J. (2011). The Energy-environment Nexus: Aerosol Science and Technology Enabling Solutions. *Front. Environ. Sci. Eng.* 5: 299–312.

Blankenship, R.E., Tiede, D.M., Barber, J., Brudvig, G.W., Fleming, G., Ghirardi, M., Gunner, M.R., Junge, W., Kramer, D.M., Melis, A., Moore, T.A., Moser, C.C., Nocera, D.G., Nozik, A.J., Ort, D.R., Parson, W.W., Prince, R.C. and Sayre, R.T. (2011). Comparing Photosynthetic and Photovoltaic Efficiencies and Recognizing the Potential for Improvement. *Science* 332: 805–809.

Bruckmeier, C., Lehenmeier, M.W., Reithmeier, R., Rieger, B., Herranz, J. and Kavakli, C. (2012). Binuclear Rhenium(I) Complexes for the Photocatalytic Reduction of CO_2. *Dalton Trans.* 41: 5026–5037.

Cao, L., Sahu, S., Anilkumar, P., Bunker, C E., Xu, J.A., Fernando, K.A.S., Wang, P., Guliants, E.A., Tackett, K.N. and Sun, Y.P. (2011). Carbon Nanoparticles as Visible-Light Photocatalysts for Efficient CO_2 Conversion and Beyond. *J. Am. Chem. Soc.* 133: 4754–4757.

Carlson, B., Leschkies, K., Aydil, E.S. and Zhu, X.Y. (2008). Valence Band Alignment at Cadmium Selenide Quantum Dot and Zinc Oxide (101) Interfaces. *J. Phys. Chem. C* 112: 8419–8423.

Chae, S.R., Hwang, E.J. and Shin, H.S. (2006). Single Cell Protein Production of Euglena Gracilis and Carbon Dioxide Fixation in an Innovative Photo-bioreactor. *Bioresour. Technol.* 97: 322–329.

Chaudhary, Y.S., Woolerton, T.W., Allen, C.S., Warner, J.H., Pierce, E., Ragsdale, S.W. and Armstrong, F.A. (2012). Visible Light-driven CO_2 Reduction by Enzyme Coupled CdS Nanocrystals. *Chem. Commun.* 48: 58–60.

Chauvin, J., Lafolet, F., Chardon-Noblat, S., Deronzier, A., Jakonen, M. and Haukka, M. (2011). Towards New Molecular Photocatalysts for CO_2 Reduction: Photo-Induced Electron Transfer versus CO Dissociation within $[Os(NN)(CO)_2Cl_2]$ Complexes. *Chem. Eur. J.* 17: 4313–4322.

Cheng, L.H., Zhang, L., Chen, H.L. and Gao, C.J. (2006). Carbon Dioxide Removal from Air by Microalgae Cultured in a Membrane-photobioreactor. *Sep. Purif. Technol.* 50: 324–329.

Chikata, Y., Kita, K., Nishimura, T., Nagashio, K. and Toriumi, A. (2013). Quantitative Characterization of Band-Edge Energy Positions in High-k Dielectrics by X-ray Photoelectron Spectroscopy. *Jpn. J. Appl. Phys.* 52: 021101.

Chiu, S.Y., Kao, C.Y., Chen, C.H., Kuan, T.C., Ong, S.C. and Lin, C.S. (2008). Reduction of CO_2 by a High-density Culture of Chlorella sp in a Semicontinuous Photobioreactor. *Bioresour. Technol.* 99: 3389–3396.

Chiu, S.Y., Tsai, M.T., Kao, C.Y., Ong, S.C. and Lin, C.S. (2009). The Air-lift Photobioreactors with Flow Patterning for High-density Cultures of Microalgae and Carbon Dioxide Removal. *Eng. Life Sci.* 9: 254–260.

Chueh, W.C. and Haile, S.M. (2009). Ceria as a Thermochemical Reaction Medium for Selectively Generating Syngas or Methane from H_2O and CO_2. *ChemSusChem* 2: 735–739.

de Jongh, P.E., Vanmaekelbergh, D. and Kelly, J.J. (1999). Cu_2O: A Catalyst for the Photochemical Decomposition of Water? *Chem. Commun.* 12: 1069–1070.

de Morais, M.G. and Costa, J.A.V. (2007a). Biofixation of Carbon Dioxide by Spirulina sp. and Scenedesmus Obliquus Cultivated in a Three-stage Serial Tubular Photobioreactor. *J. Biotechnol.* 129: 439–445.

de Morais, M.G. and Costa, J.A.V. (2007b). Carbon Dioxide Fixation by Chlorella Kessleri, C-vulgaris, Scenedesmus Obliquus and Spirulina sp. Cultivated in Flasks and Vertical Tubular Photobioreactors. *Biotechnol. Lett.* 29: 1349–1352.

de Morais, M.G. and Costa, J.A.V. (2007c). Isolation and

Selection of Microalgae from Coal Fired Thermoelectric Power Plant for Biofixation of Carbon Dioxide. *Energy Convers. Manage* 48: 2169–2173.

Dorner, R.W., Hardy, D.R., Williams, F.W. and Willauer, H.D. (2010). Heterogeneous Catalytic CO_2 Conversion to Value-added Hydrocarbons. *Energy Environ. Sci.* 3: 884–890.

Ettedgui, J., Diskin-Posner, Y., Weiner, L. and Neumann, R. (2011). Photoreduction of Carbon Dioxide to Carbon Monoxide with Hydrogen Catalyzed by a Rhenium(I) Phenanthroline-Polyoxometalate Hybrid Complex. *J. Am. Chem. Soc.* 133: 188–190.

Fan, L.H., Zhang, Y.T., Zhang, L. and Chen, H.L. (2008). Evaluation of a Membrane-sparged Helical Tubular Photobioreactor for Carbon Dioxide Biofixation by Chlorella Vulgaris. *J. Membr. Sci.* 325: 336–345.

Freund, H.J. and Roberts, M.W. (1996). Surface Chemistry of Carbon Dioxide. *Surf. Sci. Rep.* 25: 225–273.

Fujishima, A., Zhang, X.T. and Tryk, D.A. (2008). TiO_2 Photocatalysis and Related Surface Phenomena. *Surf. Sci. Rep.* 63: 515–582.

Fujita, E. (1999). Photochemical Carbon Dioxide Reduction with Metal Complexes. *Coord. Chem. Rev.* 185–6: 373–384.

Ge, L., Xu, M.X. and Fang, H.B. (2006). Preparation and Characterization of Silver and Indium Vanadate Co-doped TiO_2 Thin Films as Visible-light-activated Photocatalyst. *J. Sol-Gel Sci. Technol.* 40: 65–73.

Hamadanian, M., Reisi-Vanani, A. and Majedi, A. (2009). Preparation and Characterization of S-doped TiO_2 Nanoparticles, Effect of Calcination Temperature and Evaluation of Photocatalytic Activity. *Mater. Chem. Phys.* 116: 376–382.

Hartman, K. and Hisatsune, I.C. (1966). Infrared Spectrum of Carbon Dioxide Anion Radical. *J. Chem. Phys.* 44: 1913–1918.

Hirose, T., Maeno, Y. and Himeda, Y. (2003). Photocatalytic Carbon Dioxide Photoreduction by $Co(bpy)_3^{2+}$ Sensitized by $Ru(bpy)_3^{2+}$ Fixed to Cation Exchange Polymer. *J. Mol. Catal. A: Chem.* 193: 27–32.

Ho, S.H., Chen, W.M. and Chang, J.S. (2010). Scenedesmus Obliquus CNW-N as a Potential Candidate for CO_2 Mitigation and Biodiesel Production. *Bioresour. Technol.* 101: 8725–8730.

Ho, S.H., Chen, C.Y., Lee, D.J. and Chang, J.S. (2011). Perspectives on Microalgal CO_2-emission Mitigation Systems - A Review. *Biotechnol. Adv.* 29: 189–198.

Hong, J.D., Zhang, W., Ren, J. and Xu, R. (2013). Photocatalytic Reduction of CO_2: A Brief Review on Product Analysis and Systematic Methods. *Anal. Methods* 5: 1086–1097.

Hori, H., Koike, K., Suzuki, Y., Ishizuka, M., Tanaka, J., Takeuchi, K. and Sasaki, Y. (2002). High-pressure Photocatalytic Reduction of Carbon Dioxide Using $[fac\text{-}Re(bpy)(CO)_3P(OiPr)_3]^+$ (bpy=2,2-bipyridine). *J. Mol. Catal. A: Chem.* 179: 1–9.

Hurum, D.C., Agrios, A.G., Gray, K.A., Rajh, T. and Thurnauer, M.C. (2003). Explaining the Enhanced Photocatalytic Activity of Degussa P25 Mixed-phase TiO_2 Using EPR. *J. Phys. Chem. B* 107: 4545–4549.

Ikeue, K., Nozaki, S., Ogawa, M. and Anpo, M. (2002). Photocatalytic Reduction of CO_2 with H_2O on Ti-Containing Porous Silica Thin Film Photocatalysts. *Catal. Lett.* 80: 111–114.

Indrakanti, V.P., Kubicki, J.D. and Schobert, H.H. (2009). Photoinduced Activation of CO_2 on Ti-based Heterogeneous Catalysts: Current State, Chemical Physics-based Insights and Outlook. *Energy Environ. Sci.* 2: 745–758.

Inoue, T., Fujishima, A., Konishi, S. and Honda, K. (1979). Photoelectrocatalytic Reduction of Carbon Dioxide in Aquesous Suspensions of Semiconductor Powders. *Nature* 277: 637.

Inoue, H., Yamachika, M. and Yoneyama, H. (1992). Photocatalytic Conversion of Lactic-Acid to Malic-Acid through Pyruvic-Acid in the Presence of Malic Enzyme and Semiconductor Photocatalysts. *J. Chem. Soc., Faraday Trans.* 88: 2215–2219.

Jacob-Lopes, E., Revah, S., Hernandez, S., Shirai, K. and Franco, T.T. (2009a). Development of Operational Strategies to Remove Carbon Dioxide in Photobioreactors. *Chem. Eng. J.* 153: 120–126.

Jacob-Lopes, E., Scoparo, C.H.G., Lacerda, L.M.C.F. and Franco, T.T. (2009b). Effect of Light Cycles (Night/Day) on CO_2 Fixation and Biomass Production by Microalgae in Photobioreactors. *Chem. Eng. Process.* 48: 306–310.

Jin, H.F., Lim, B.R. and Lee, K. (2006). Influence of Nitrate Feeding on Carbon Dioxide Fixation by Microalgae. *J. Environ. Sci. Health., Part A* 41: 2813–2824.

Jitaru, M., Lowy, D.A., Toma, M., Toma, B.C. and Oniciu, L. (1997). Electrochemical Reduction of Carbon Dioxide on Flat Metallic Cathodes. *J. Appl. Electrochem.* 27: 875–889.

Kaneco, S., Shimizu, Y., Ohta, K. and Mizuno, T. (1998). Photocatalytic Reduction of High Pressure Carbon Dioxide Using TiO_2 Powders with a Positive Hole Scavenger. *J. Photochem. Photobiol., A* 115: 223–226.

Kaneco, S., Kurimoto, H., Shimizu, Y., Ohta, K. and Mizuno, T. (1999). Photocatalytic Reduction of CO_2 Using TiO_2 Powders in Supercritical Fluid CO_2. *Energy* 24: 21–30.

Khenkin, A.M., Efremenko, I., Weiner, L., Martin, J.M.L. and Neumann, R. (2010). Photochemical Reduction of Carbon Dioxide Catalyzed by a Ruthenium-Substituted Polyoxometalate. *Chem. Eur. J.* 16: 1356–1364.

Kim, W., Seok, T. and Choi, W. (2012). Nafion Layer-enhanced Photosynthetic Conversion of CO_2 into Hydrocarbons on TiO_2 Nanoparticles. *Energy Environ. Sci.* 5: 6066–6070.

Kitano, M., Matsuoka, M., Ueshima, M. and Anpo, M. (2007). Recent Developments in Titanium Oxide-based Photocatalysts. *Appl. Catal., A* 325: 1–14.

Koffyberg, F.P. and Benko, F.A. (1982). A Photo-Electrochemical Determination of the Position of the Conduction and Valence Band Edges of P-Type Cuo. *J. Appl. Phys.* 53: 1173–1177.

Kohno, Y., Hayashi, H., Takenaka, S., Tanaka, T., Funabiki, T. and Yoshida, S. (1999). Photo-enhanced Reduction of Carbon Dioxide with Hydrogen over Rh/TiO_2. *J.*

Photochem. Photobiol., A 126: 117–123.

Kohno, Y., Tanaka, T., Funabiki, T. and Yoshida, S. (2000). Photoreduction of CO_2 with H_2 over ZrO_2. A Study on Interaction of Hydrogen with Photoexcited CO_2. *Phys. Chem. Chem. Phys*. 2: 2635–2639.

Kohno, Y., Ishikawa, H., Tanaka, T., Funabiki, T. and Yoshida, S. (2001). Photoreduction of Carbon Dioxide by Hydrogen over Magnesium Oxide. *Phys. Chem. Chem. Phys.* 3: 1108–1113.

Ku, Y., Lee, W.H. and Wang, W.Y. (2004). Photocatalytic Reduction of Carbonate in Aqueous Solution by UV/TiO_2 Process. *J. Mol. Catal. A: Chem.* 212: 191–196.

Kumar, A., Ergas, S., Yuan, X., Sahu, A., Zhang, Q.O., Dewulf, J., Malcata, F.X. and van Langenhove, H. (2010). Enhanced CO_2 Fixation and Biofuel Production via Microalgae: Recent Developments and Future Directions. *Trends Biotechnol.* 28: 371–380.

Kurano, N., Ikemoto, H., Miyashita, H., Hasegawa, T., Hata, H. and Miyachi, S. (1995). Fixation and Utilization of Carbon-Dioxide by Microalgal Photosynthesis. *Energy Convers. Manage* 36: 689–692.

Lehn, J.M. and Ziessel, R. (1982). Photochemical Generation of Carbon Monoxide and Hydrogen by Reduction of Carbon Dioxide and Water under Visible Light Irradiation. *Proc. Nat. Acad. Sci. U.S.A.* 79: 701–704.

Li, G.L., Li, W.X. and Li, C. (2010a). Model Relation between the Energy-band Edge and the Fermi Level of the Nondegenerate Semiconductor TiO_2: Application to Electrochemistry. *Phys. Rev. B* 82: 235109.

Li, H.X., Bian, Z.F., Zhu, J., Huo, Y.N., Li, H. and Lu, Y.F. (2007). Mesoporous Au/TiO_2 Nanocomposites with Enhanced Photocatalytic Activity. *J. Am. Chem. Soc.* 129: 4538.

Li, P., Ouyang, S.X., Xi, G.C., Kako, T. and Ye, J.H. (2012a). The Effects of Crystal Structure and Electronic Structure on Photocatalytic H_2 Evolution and CO_2 Reduction over Two Phases of Perovskite-Structured $NaNbO_3$. *J. Phys. Chem. C* 116: 7621–7628.

Li, X., Liu, H.L., Luo, D.L., Li, J.T., Huang, Y., Li, H.L., Fang, Y.P., Xu, Y.H. and Zhu, L. (2012b). Adsorption of CO_2 on Heterostructure CdS(Bi_2S_3)/TiO_2 Nanotube Photocatalysts and Their Photocatalytic Activities in the Reduction of CO_2 to Methanol under Visible Light Irradiation. *Chem. Eng. J.* 180: 151–158.

Li, Y., Wang, W.N., Zhan, Z.L., Woo, M.H., Wu, C.Y. and Biswas, P. (2010b). Photocatalytic Reduction of CO_2 with H_2O on Mesoporous Silica Supported Cu/TiO_2 Catalysts. *Appl. Catal., B* 100: 386–392.

Linsebigler, A.L., Lu, G.Q. and Yates, J.T. (1995). Photocatalysis on TiO_2 Surfaces - Principles, Mechanisms, and Selected Results. *Chem. Rev.* 95: 735–758.

Liu, B.J., Torimoto, T. and Yoneyama, H. (1998). Photocatalytic Reduction of CO_2 Using Surface-modified CdS Photocatalysts in Organic Solvents. *J. Photochem. Photobiol., A* 113: 93–97.

Liu, L.J., Zhao, H.L., Andino, J.M. and Li, Y. (2012). Photocatalytic CO_2 Reduction with H_2O on TiO_2 Nanocrystals: Comparison of Anatase, Rutile, and Brookite Polymorphs and Exploration of Surface Chemistry. *ACS Catal.* 2: 1817–1828.

Liu, L.J., Zhao, C., Zhao, H.L., Pitts, D., and Li, Y. (2013). Porous Microshperes of MgO-patched TiO_2 for CO_2 Photoreduction with H_2O Vapor: Temperature-dependent Activity and Stability. *Chem. Commun*. 49: 3664–3666.

Liu, S.H., Zhao, Z.H. and Wang, Z.Z. (2007). Photocatalytic Reduction of Carbon Dioxide Using Sol-gel Derived Titania-supported CoPc Catalysts. *Photochem. Photobiol. Sci.* 6: 695–700.

Lo, C.C., Hung, C.H., Yuan, C.S. and Wu, J.F. (2007). Photoreduction of Carbon Dioxide with H_2 and H_2O over TiO_2 and ZrO_2 in a Circulated Photocatalytic Reactor. *Sol. Energy Mater. Sol. Cells* 91: 1765–1774.

Lopez, C.V.G., Fernandez, F.G.A., Sevilla, J.M.F., Fernandez, J.F.S., Garcia, M.C.C. and Grima, E.M. (2009). Utilization of the Cyanobacteria Anabaena sp ATCC 33047 in CO_2 Removal Processes. *Bioresour. Technol.* 100: 5904–5910.

Matsumoto, Y. (1996). Energy Positions of Oxide Semiconductors and Photocatalysis with Iron Complex Oxides. *J. Solid State Chem.* 126: 227–234.

Metz, B., Davidson, O., de Coninck, H., Loos, M. and Meyer, C. (2005). *IPCC Special Report on Carbon Dioxide Capture and Storage*, New York.

Morris, A.J., Meyer, G.J. and Fujita, E. (2009). Molecular Approaches to the Photocatalytic Reduction of Carbon Dioxide for Solar Fuels. *Acc. Chem. Res.* 42: 1983–1994.

Murakami, M. and Ikenouchi, M. (1997). The Biological CO_2 Fixation and Utilization Project by RITE .2. Screening and Breeding of Microalgae with High Capability in Fixing CO_2. *Energy Convers. Manage* 38: S493–S497.

Navalon, S., Dhakshinamoorthy, A., Alvaro, M. and Garcia, H. (2013). Photocatalytic CO_2 Reduction Using Non-Titanium Metal Oxides and Sulfides. *ChemSusChem* 6: 562–577.

Negoro, M., Shioji, N., Miyamoto, K. and Miura, Y. (1991). Growth of Microalgae in High CO_2 Gas and Effects of SO_x and NO_x. *Appl. Biochem. Biotechnol.* 28–29: 877–886.

Pan, J., Wu, X., Wang, L.Z., Liu, G., Lub, G.Q. and Cheng, H.M. (2011). Synthesis of Anatase TiO_2 Rods with Dominant Reactive {010} Facets for the Photoreduction of CO_2 to CH_4 and Use in Dye-sensitized Solar cells. *Chem. Commun.* 47: 8361–8363.

Perissinotti, L.L., Brusa, M.A. and Grela, M.A. (2001). Yield of Carboxyl Anion Radicals in the Photocatalytic Degradation of Formate over TiO_2 particles. *Langmuir* 17: 8422–8427.

Praus, P., Kozak, O., Koci, K., Panacek, A. and Dvorsky, R. (2011). CdS Nanoparticles Deposited on Montmorillonite: Preparation, Characterization and Application for Photoreduction of Carbon Dioxide. *J. Colloid Interface Sci.* 360: 574–579.

Roy, S.C., Varghese, O.K., Paulose, M. and Grimes, C.A. (2010). Toward Solar Fuels: Photocatalytic Conversion of Carbon Dioxide to Hydrocarbons. *ACS Nano* 4: 1259–1278.

Ryu, H.J., Oh, K.K. and Kim, Y.S. (2009). Optimization of

the Influential Factors for the Improvement of CO_2 Utilization Efficiency and CO_2 Mass Transfer Rate. *J. Ind. Eng. Chem.* 15: 471–475.

Sakai, N., Sakamoto, Y., Kishimoto, N., Chihara, M. and Karube, I. (1995). Chlorella Strains from Hot-Springs Tolerant to High-Temperature and High CO_2. *Energy Convers. Manage* 36: 693–696.

Sathish, M., Viswanathan, B., Viswanath, R.P. and Gopinath, C.S. (2005). Synthesis, Characterization, Electronic Structure, and Photocatalytic Activity of Nitrogen-doped TiO_2 Nanocatalyst. *Chem. Mater.* 17: 6349–6353.

Scragg, A.H., Illman, A.M., Carden, A. and Shales, S.W. (2002). Growth of Microalgae with Increased Calorific Values in a Tubular Bioreactor. *Biomass Bioenergy* 23: 67–73.

Song, C.S. (2006). Global Challenges and Strategies for Control, Conversion and Utilization of CO_2 for Sustainable Development Involving Energy, Catalysis, Adsorption and Chemical Processing. *Catal. Today* 115: 2–32.

Sung, K.D., Lee, J.S., Shin, C.S. and Park, S.C. (1999). Isolation of a New Highly CO_2 Tolerant Fresh Water Microalga Chlorella sp. KR-1. *Renewable Energy* 16: 1019–1022.

Sutin, N., Creutz, C. and Fujita, E. (1997). Photo-induced Generation of Dihydrogen and Reduction of Carbon Dioxide Using Transition Metal Complexes. *Comments Inorg. Chem.* 19: 67–92.

Takeda, H., Koike, K., Inoue, H. and Ishitani, O. (2008). Development of an Efficient Photocatalytic System for CO_2 Reduction Using Rhenium(l) Complexes Based on Mechanistic Studies. *J. Am. Chem. Soc.* 130: 2023–2031.

Tseng, I.H., Chang, W.C. and Wu, J.C.S. (2002). Photoreduction of CO_2 Using Sol-gel Derived Titania and Titania-supported Copper Catalysts. *Appl. Catal., B* 37: 37–48.

Tseng, I.H., Wu, J.C.S. and Chou, H.Y. (2004). Effects of Sol-gel Procedures on the Photocatalysis of Cu/TiO_2 in CO_2 Photoreduction. *J. Catal.*. 221: 432–440.

Tu, W.G., Zhou, Y., Liu, Q., Tian, Z.P., Gao, J., Chen, X.Y., Zhang, H.T., Liu, J.G. and Zou, Z.G. (2012). Robust Hollow Spheres Consisting of Alternating Titania Nanosheets and Graphene Nanosheets with High Photocatalytic Activity for CO_2 Conversion into Renewable Fuels. *Adv. Funct. Mater.* 22: 1215–1221.

Usubharatana, P., McMartin, D., Veawab, A. and Tontiwachwuthikul, P. (2006). Photocatalytic Process for CO_2 Emission Reduction from Industrial Flue Gas Streams. *Ind. Eng. Chem. Res.* 45: 2558–2568.

Varghese, O.K., Paulose, M., LaTempa, T.J. and Grimes, C.A. (2009). High-Rate Solar Photocatalytic Conversion of CO_2 and Water Vapor to Hydrocarbon Fuels. *Nano Lett.* 9: 731–737.

Wang, C.J., Thompson, R.L., Ohodnicki, P., Baltrus, J. and Matranga, C. (2011b). Size-dependent Photocatalytic Reduction of CO_2 with PbS Quantum Dot Sensitized TiO_2 Heterostructured Photocatalysts. *J. Mater. Chem.* 21: 13452–13457.

Wang, C., Xie, Z.G., deKrafft, K.E. and Lin, W.L. (2011a). Doping Metal-Organic Frameworks for Water Oxidation, Carbon Dioxide Reduction, and Organic Photocatalysis. *J. Am. Chem. Soc.* 133: 13445–13454.

Wang, P.Q., Bai, Y., Liu, J.Y., Fan, Z. and Hu, Y.Q. (2012a). One-pot Synthesis of Rutile TiO_2 Nanoparticle Modified Anatase TiO_2 Nanorods Toward Enhanced Photocatalytic Reduction of CO_2 into Hydrocarbon Fuels. *Catal. Commun.* 29: 185–188.

Wang, W.N., An, W.J., Ramalingam, B., Mukherjee, S., Niedzwiedzki, D.M., Gangopadhyay, S. and Biswas, P. (2012b). Size and Structure Matter: Enhanced CO_2 Photoreduction Efficiency by Size-Resolved Ultrafine Pt Nanoparticles on TiO_2 Single Crystals. *J. Am. Chem. Soc.* 134: 11276–11281.

Wang, W.N., Park, J. and Biswas, P. (2011c). Rapid Synthesis of Nanostructured $Cu\text{-}TiO_2\text{-}SiO_2$ Composites for CO_2 Photoreduction by Evaporation Driven Self-assembly. *Catal. Sci. Technol.* 1: 593–600.

Windle, C.D. and Perutz, R.N. (2012). Advances in Molecular Photocatalytic and Electrocatalytic CO_2 Reduction. *Coord. Chem. Rev.* 256: 2562–2570.

Woolerton, T.W., Sheard, S., Reisner, E., Pierce, E., Ragsdale, S.W. and Armstrong, F.A. (2010). Efficient and Clean Photoreduction of CO_2 to CO by Enzyme-Modified TiO_2 Nanoparticles Using Visible Light. *J. Am. Chem. Soc.* 132: 2132–2133.

Woolerton, T.W., Sheard, S., Chaudhary, Y.S. and Armstrong, F.A. (2012). Enzymes and Bio-inspired Electrocatalysts in Solar Fuel Devices. *Energy Environ. Sci.* 5: 7470–7490.

Wu, J.C.S. (2009). Photocatalytic Reduction of Greenhouse Gas CO_2 to Fuel. *Catal. Surv. Asia* 13: 30–40.

Xia, X.H., Jia, Z.H., Yu, Y., Liang, Y., Wang, Z. and Ma, L.L. (2007). Preparation of Multi-walled Carbon Nanotube Supported TiO_2 and Its Photocatalytic Activity in the Reduction of CO_2 with H_2O. *Carbon* 45: 717–721.

Xu, H., Ouyang, S., Li, P., Kato, T. and Ye, J. (2013). High-Active Anatase TiO_2 Nanosheets Exposed with 95% {100} Facets Toward Efficient H_2 Evolution and CO_2 Photoreduction. *ACS Appl. Mater. Interfaces* 5: 1348–1354.

Xu, Y. and Schoonen, M.A.A. (2000). The Absolute Energy Positions of Conduction and Valence Bands of Selected Semiconducting Minerals. *Am. Mineral.* 85: 543–556.

Yadav, R.K., Baeg, J.O., Oh, G.H., Park, N.J., Kong, K.J., Kim, J., Hwang, D.W. and Biswas, S.K. (2012). A Photocatalyst-Enzyme Coupled Artificial Photosynthesis System for Solar Energy in Production of Formic Acid from CO_2. *J. Am. Chem. Soc.* 134: 11455–11461.

Yahaya, A.H., Gondal, M.A. and Hameed, A. (2004). Selective Laser Enhanced Photocatalytic Conversion Of CO_2 into Methanol. *Chem. Phys. Lett.* 400: 206–212.

Yamashita, H., Fujii, Y., Ichihashi, Y., Zhang, S.G., Ikeue, K., Park, D.R., Koyano, K., Tatsumi, T. and Anpo, M. (1998). Selective Formation of CH_3OH in the Photocatalytic Reduction of CO_2 with H_2O on Titanium Oxides Highly Dispersed within Zeolites and Mesoporous Molecular Sieves. *Catal. Today* 45: 221–227.

Yoo, C., Jun, S.Y., Lee, J.Y., Ahn, C.Y. and Oh, H.M. (2010). Selection of Microalgae for Lipid Production

under High Levels Carbon Dioxide. *Bioresour. Technol.* 101: S71–S74.

Yu, J.C., Yu, J.G., Ho, W.K., Jiang, Z.T. and Zhang, L.Z. (2002). Effects of F^- Doping on the Photocatalytic Activity and Microstructures of Nanocrystalline TiO_2 Powders. *Chem. Mater.* 14: 3808–3816.

Yuan, Y.J., Yu, Z.T., Zhang, J.Y. and Zou, Z.G. (2012). A Copper(I) Dye-sensitised TiO_2-based System for Efficient Light Harvesting and Photoconversion of CO_2 into Hydrocarbon Fuel. *Dalton T.* 41: 9594–9597.

Zeng, X.H., Danquah, M.K., Chen, X.D. and Lu, Y.H. (2011). Microalgae Bioengineering: From CO_2 Fixation to Biofuel Production. *Renewable Sustainable Energy Rev.* 15: 3252–3260.

Zhao, H., Liu, L., Andino, J.M. and Li, Y. (2013). Bicrystalline TiO_2 with Controllable Anatase-brookite Phase Content for Enhanced CO_2 Photoreduction to Fuels. *J. Mater. Chem. A* 1: 8209–8216.

Received for review, September 25, 2013
Accepted, October 7, 2013